J Am Soc Nephrol 10: 444–457, 1999

Osteopontin Expression in Fetal and Mature Human Kidney

KELLY L. HUDKINS,* CECILIA M. GIACHELLI,* YAN CUI,*
WILLIAM G. COUSER,† RICHARD J. JOHNSON,† and CHARLES E. ALPERS*
**Department of Pathology and †Division of Nephrology, Department of Medicine, University of Washington School of Medicine, Seattle, Washington.*

Abstract. Osteopontin is a secreted phosphoprotein that is expressed by normal kidney, and has been associated with a number of functions including cell adhesion, migration, signaling, and biomineralization. Although there is a vast literature detailing osteopontin localization in various rodent models of both development and disease, this article presents the first comprehensive description of osteopontin localization in human kidney. In this study, immunohistochemistry, immunoelectron microscopy, *in situ* hybridization, and Northern blotting are used to analyze osteopontin protein and mRNA expression in human fetal and normal mature renal tissue. Osteopontin is expressed in the human embryonic renal tubular epithelium beginning on approximately day 75 to 80 of gestation. In the fetal kidney, osteopontin can also be seen occasionally expressed in the ureteric buds and in some interstitial cells. As localized at the protein and mRNA level, the tubular expression of osteopontin increases with increasing gestational age and persists into adulthood. In the normal adult kidney, osteopontin is localized primarily to the distal nephron and is strongly expressed by the thick ascending limb of the loops of Henle. Osteopontin expression can also be observed in some collecting duct epithelium. In cases that exhibit foci of interstitial fibrosis and an associated influx of interstitial macrophages, osteopontin expression is significantly upregulated in all tubular segments, including proximal tubules.

Osteopontin is a secreted phosphoprotein that was originally isolated from demineralized rat bone and was thought to be a bone-specific protein. More recently, it has been shown to be expressed in a number of different tissues, including kidney, lung, liver, bladder, pancreas, and breast (1,2). Its expression has also been demonstrated in vascular smooth muscle cells and macrophages *in vitro* and *in vivo* (3–5). Osteopontin has been known by a number of different names, depending on the investigator and site of action observed, such as rat bone sialoprotein I (6), Eta-1 (early T lymphocyte activation gene 1) (7), urinary stone protein (8), uropontin (9), and 2ar (10). Thus, osteopontin appears to be a very multifunctional protein (11,12).

Osteopontin contains an arginine-glycine-aspartate (RGD) binding sequence and is known to bind to a number of integrins, including $\alpha v\beta 3$ (13), $\alpha v\beta 5$ (13), and $\alpha v\beta 1$ (14), as well as CD44, the hyaluronan receptor (15). Binding of osteopontin to the integrin $\alpha v\beta 3$ appears to mediate both metanephric tubulogenesis (16) and the adhesion and migration of vascular smooth muscle cells (17,18).

There is an increasing body of evidence that identifies osteopontin as an important mediator of tubulointerstitial injury in a variety of rodent renal injury models, including ureteral obstruction, angiotensin II infusion, cyclosporine nephrotoxicity, passive Heyman nephritis, and the Thy-1 model of mesangial proliferative nephropathy (19–23). In these models, expression of osteopontin has been identified in renal tubules, and upregulated tubular expression has been specifically linked to local accumulations of monocytic cells.

Although there are a number of descriptions of the expression of osteopontin in rodent kidney tissue (10,19–22,24–28), and it is known to be expressed in human kidney (1), its precise localization in normal adult human kidney has not been well characterized. This study presents the first description of osteopontin localization in human fetal kidney and the first comprehensive description of osteopontin localization in normal human kidney. This study was undertaken as part of an effort to extend observations made in rodent injury models to investigations of human disease. As a first step in that process, we sought to establish that osteopontin exhibits a similar pattern of expression in human tissue. In this study, we used immunocytochemistry, *in situ* hybridization, and Northern blotting to determine the location of osteopontin protein and mRNA in developing and mature adult human kidney tissue. We also used double immunocytochemistry to colocalize osteopontin with both epithelial membrane antigen (EMA) and sodium potassium ATPase (Na,K-ATPase). EMA is known to be expressed by distal convoluted tubules, collecting duct, and the thick ascending limb of the loop of Henle (29,30), as is Na,K-ATPase (31,32).

In human fetal kidney, osteopontin is expressed predominantly by the ureteric bud and tubular structures. Expression of osteopontin by adult human kidney is most often localized to distal tubular segments, and the degree of tubular expression appears to correlate with the number of macrophage/mono-

Received June 15, 1998. Accepted September 21, 1998.
Correspondence to Dr. Charles E. Alpers, University of Washington Medical Center, Department of Pathology, Box 356100, 1959 NE Pacific Avenue, Seattle, WA 98195. Phone: (206) 548-6409; Fax: (206) 548-4928; E-mail: calp@u.washington.edu

1046-6673/1003-0444$03.00/0
Journal of the American Society of Nephrology

cytes present in the tissue. These findings suggest that knowledge gained from studies of osteopontin localization and its association with monocyte/macrophages that has been obtained from experimental models in rodents is likely to be applicable to our understanding of human disease.

Materials and Methods

Tissue

Mature human kidney tissue was obtained from macroscopically normal portions of kidneys resected for localized neoplasms. The patients ranged in age from 32 to 85 yr old. Human fetal kidneys (estimated gestational age 54 to 127 d) were collected from tissue examined after therapeutic abortions. Tissue specimens were fixed either in methyl Carnoy's solution (adults $n = 24$; fetal $n = 25$;) as described previously (33) or 10% neutral-buffered formalin (adults $n = 24$; fetals $n = 14$). All fixed tissues were processed and embedded in paraffin according to standard protocols.

Antibodies

LF7 is a rabbit polyclonal antibody directed against the intact osteopontin protein molecule isolated from bone (34). Its specific recognition of osteopontin has been characterized by Western blotting, and its ability to detect osteopontin by immunocytochemistry in fixed tissue sections has been demonstrated previously (17). Further demonstration of the specificity of this antibody comes from previous complementary studies that localize expression of osteopontin mRNA to sites of peptide expression in tissue sections. In addition, we used a goat polyclonal antibody, OP199, specific for rat osteopontin, which also cross-reacts with human osteopontin protein. Its specificity for osteopontin has been characterized by Western blotting (18). Both antibodies demonstrated identical patterns of staining. We therefore chose one of these reagents, LF7, because of its wider use in previously published studies by ourselves and others, to perform most of the immunohistochemical procedures described in this article.

PGM1 (Dako, Carpinteria, CA) is a well characterized murine monoclonal antibody directed against the CD68 epitope present on human monocytes and macrophages. Its specificity has been demonstrated by Western blotting, and it has been shown to be reactive in formalin-fixed, paraffin-embedded tissue (35).

1A4 (Dako) is a murine monoclonal antibody specific for α-smooth muscle actin (36). It has been extensively characterized by Western blotting, and previously shown to identify smooth muscle actin in methyl Carnoy's and formalin-fixed tissue using immunohistochemical procedures (33,37).

EMA clone E29 (Dako) is a mouse monoclonal IgG2a that is specific for epithelial membrane antigen (38). It reacts with normal epithelium in a variety of tissues, and has been characterized by comparative immunocytochemistry with several other polyclonal and monoclonal anti-EMA antibodies (38).

Rabbit anti-Na,K-ATPase (Upstate Biotechnology, Lake Placid, NY) is a whole rabbit antiserum created against the β-1 subunit of rat Na,K-ATPase (39). It has been characterized with Western blotting.

Immunohistochemistry

Methyl Carnoy's-fixed, paraffin-embedded tissue sections were deparaffinized, rehydrated, and then incubated in 3% hydrogen peroxide to block endogenous peroxidases. The sections were then incubated sequentially with 10% normal serum (only used for polyclonal antibodies to block nonspecific binding), primary antibody, biotinylated secondary antibody (Vector Laboratories, Burlingame, CA), and the avidin-biotin-horseradish peroxidase (HRP) complex (ABC; Vector). The sections were then visualized with 3, 3′- diaminobenzidine (DAB; Sigma, St. Louis, MO) with nickel chloride enhancement to give a black-brown reaction product. After methyl green counterstaining, the slides were dehydrated and coverslipped. For all samples, negative controls for the immunohistochemistry included substituting for the primary antibody an irrelevant IgG from the same species or phosphate-buffered saline (PBS).

Quantification was performed at a magnification of $\times$400. Ten random fields within the cortex were counted for each case studied. The data are presented as the percentage of all tubular segments positive for osteopontin expression. The number of CD68-positive cells was counted as described previously (40), and the data are presented as total number of CD68-positive cells present per high-power field (HPF). Due to the often elongated morphology of monocytes/macrophages, positive cells were counted only if the nucleus was observed.

Tissue sections stained with the anti-smooth muscle actin antibody were examined in a blinded manner and assigned a semiquantitative score, as described previously (33).The grading scale is as follows: 0, $<$2% interstitial staining; 1+, 2 to 10% of interstitium positively stained; 2+, 10 to 25% of interstitium positively stained; 3+, 25 to 50% of interstitium positively stained; 4+, 50 to 75% of interstitium positively stained; and 5+, 75 to 100% of interstitium positively stained.

Double immunocytochemistry was performed to detect osteopontin expression in combination with CD68 and the tubular markers EMA and Na,K-ATPase. Briefly, slides were incubated with either LF7 or CD68, peroxidase-conjugated secondary antibody, and reacted with DAB to give a brown color product. After washing, residual peroxidase blocking with hydrogen peroxide and normal serum blocking, the slides were then stained with the second primary antibody (LF7, EMA, or Na,K-ATPase), biotinylated secondary antibody, ABC-HRP (Vector), and reacted with Vector VIP peroxidase substrate kit (Vector) to give a purple reaction product. Negative controls consisted of substituting irrelevant mouse or rabbit IgG (Dako) for one of the two primary antibodies.

Immunoelectron Microscopy

Frozen, 4% paraformaldehyde-fixed kidneys were sectioned at 6 μm and air-dried on glass slides for 30 min. The sections were then stained by hydrating in PBS for 15 min, incubated in 0.05% sodium borohydride in PBS at 4°C for 60 min to reduce free aldehyde groups, rinsed, and then incubated with antibody LF7 overnight at 4°C. The slides were then washed and incubated sequentially with biotinylated goat-anti-rabbit antibody (Vector), ABC-peroxidase (Vector), and DAB. Afterward, the slides were rinsed in distilled water, reacted with 2% osmium tetroxide for 30 min, rinsed, and then dehydrated through graded ethanols and into propylene oxide. Sections were then infiltrated with PolyBed resin (Polysciences, Warrington, PA). Beem capsules were filled with PolyBed, inverted over the sections, and polymerized at 55°C for 48 h. The blocks were removed by heating the slides briefly and snapping off the capsule. Thin, 0.1-μm sections were cut, mounted on grids, and examined in a Philips 410 microscope.

In Situ Hybridization

Human osteopontin cDNA in plasmid pBluescript SK(−) (plasmid OP-10) was obtained from Dr. Larry Fisher (National Institutes of Health) (41). It contains a 1493-bp fragment of the human osteopontin gene, which includes the entire protein encoding sequence of the

human osteopontin Ia gene. This was linearized with *Xba*I and *Xho*I and then transcribed into both antisense and sense (negative control) riboprobes using reagents from Promega (Madison, WI), except ^{35}S-UTP, which was obtained from New England Nuclear (Boston, MA). The details of this procedure have been previously published (42). In addition, nonradioactive riboprobe was labeled with digoxigenin-UTP (Boehringer Mannheim, Indianapolis, IN), using the same reagents from Promega.

Fetal and adult kidney tissue, which had been fixed in 10% formalin and embedded in paraffin, was deparaffinized following standard protocol. The sections were washed with 0.5× SSC (1× SSC = 150 mM NaCl, 15 mM Na citrate, pH 7.0) and digested with 10 μg/ml proteinase K (Sigma) in Tris buffer (500 mM NaCl, 10 mM Tris, pH 8.0) for 30 min at 37°C. Several 0.5× SSC washes were followed by prehybridization for 2 h in 50 μl of prehybidization buffer (50% formamide, 0.3 M NaCl, 20 mM Tris, pH 8.0, 5 mM ethylenediaminetetra-acetic acid, 1× Denhardt's solution, 10% dextran sulfate, 10 mM dithiothreitol, 50 μg/ml yeast tRNA) at 50°C. The hybridizations were started by adding either 500,000 cpm of ^{35}S-labeled riboprobe or 1 ng/μl digoxigenin-labeled riboprobe in 50 μl of prehybridization buffer. The hybridization was allowed to proceed overnight at 50°C. After hybridization, sections were washed with 0.5× SSC, treated with RNase A (20 μg/ml, 30 min room temperature), washed in 2× SSC (2 × 2 min), followed by three high stringency washes in 0.1× SSC/0.1% Tween 20 (Sigma) at 50°C, and several 2× SSC washes.

The slides hybridized with the ^{35}S-labeled probe were dipped in NTB2 nuclear emulsion (Kodak, Rochester, NY) and exposed in the dark at 4°C for 1 to 4 wk. After developing, the sections were

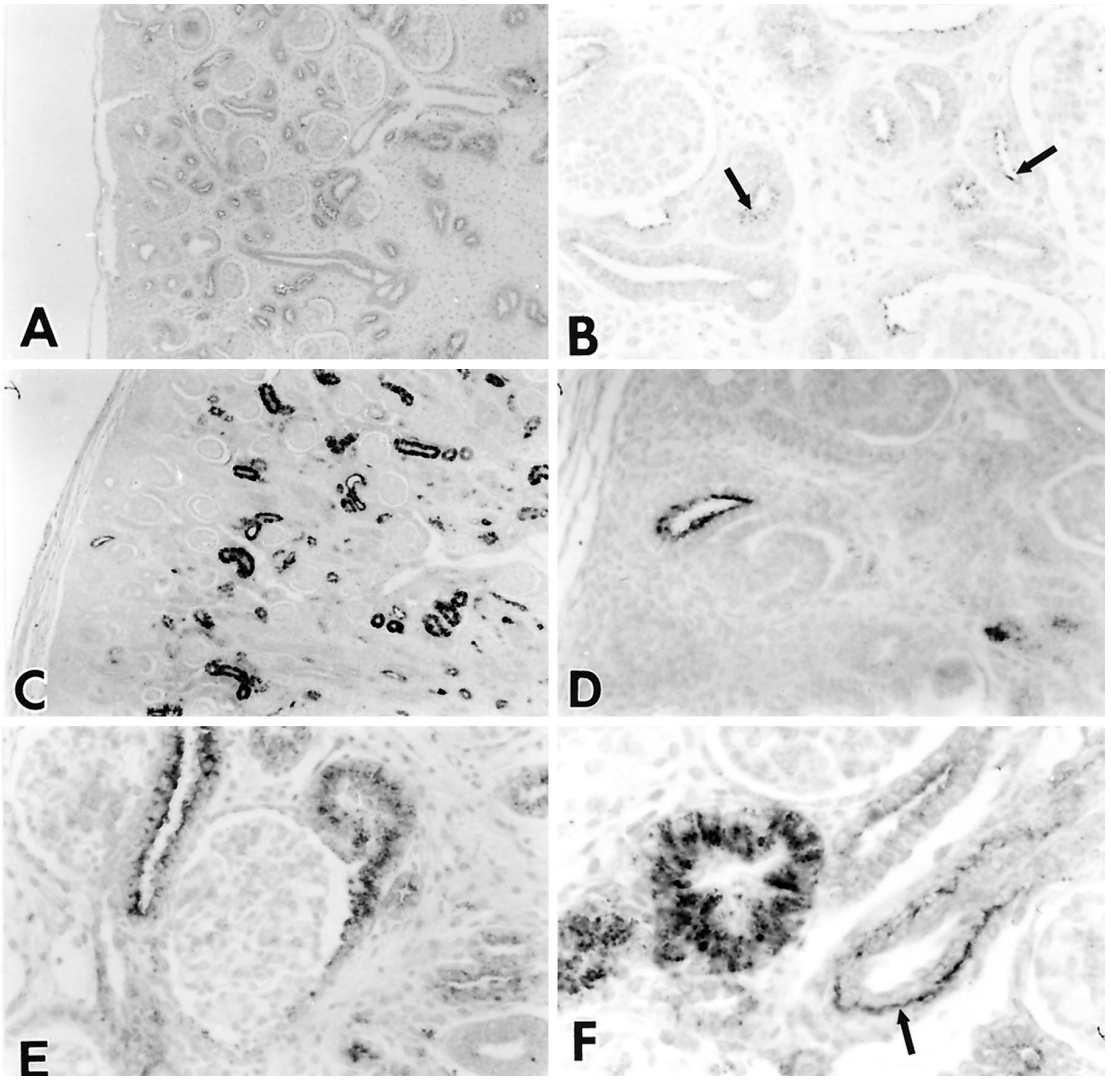

Figure 1. Expression of osteopontin in human fetal kidneys. (A) Low-power view of embryonic kidney, estimated gestation age 72 d. Focal, weak expression of osteopontin in tubular structures is undetectable at this magnification. (B) Higher power view of A, demonstrating very weak osteopontin immunoreactivity limited to the luminal surfaces of the tubular structures (arrows). (C) Low-power view of human fetal kidney, estimated gestational age 105 d, demonstrating strong, cytoplasmic expression of osteopontin in tubules. There is no expression in the blastema, comma- or S-shaped glomeruli, or the more mature glomeruli. (D) Higher power view of B showing luminal expression of osteopontin in a ureteric bud located within the metanephric blastema. (E) Osteopontin expression in a proximal tubule that is contiguous with the parietal epithelium lining Bowman's capsule of a more mature glomerulus (gestational age 89 d). (F) Mesenchymal cells of the arterial adventitia (arrow) in a kidney of gestational age 81 d, demonstrating positive osteopontin expression. Magnification: ×100 in A and C; ×400 in B and D; ×600 in E and F.

counterstained with hematoxylin and eosin, dehydrated, mounted, and viewed. Positive cellular labeling was defined as five or more silver grains concentrated over a single cell.

Hybridization with the digoxigenin-labeled probe was visualized using the tyramide signal amplification system (New England Nuclear). Briefly, after hybridization and high stringency washes, the slides were blocked with TNB buffer (New England Nuclear) for 30 min at 37°C, then incubated sequentially with anti-digoxigenin HRP, biotinyl tyramide, streptavidin-HRP, or streptavidin-alkaline phosphatase and finally visualized with DAB (with nickel chloride enhancement) or 5-bromo-4-chloro-3-indolyl phosphate/nitroblue tetrazolium (Boehringer Mannheim), respectively. Slides were counterstained with methyl green, dehydrated, and mounted. Negative controls included simultaneous hybridization performed on replicate tissue sections using the sense riboprobe.

Northern Hybridization

Biotin-labeled probes were transcribed using the Strip EZ RNA transcription kit (Ambion) and biotin-21-UTP (Clontech, Palo Alto, CA). Both the OP-10 antisense template and the pTri-28S-RNA antisense template (Ambion) were used to create probes.

Total RNA was isolated from mature human renal cortex and from whole fetal kidney using the Totally RNA kit (Ambion). Five micrograms of total RNA (as measured by ultraviolet spectrophotometry) was electrophoresed on a 1% agarose gel containing 2% formaldehyde, 40 mM MOPS (3-[*N*-morpholino] propanesulfonic acid), 10 mM sodium acetate, and 1 mM ethylenediaminetetra-acetic acid. The RNA was then vacuum-blotted to a positively charged nylon membrane, ultraviolet cross-linked, and hybridized with the biotin-labeled OP-10 probe, using NorthernMax Hybridization solution (Ambion). After overnight hybridization at 65°C and several high stringency washes, the biotin-labeled probe was detected with streptavidin conjugated to alkaline phosphatase (Ambion) and CDP Star (Tropix, Bedford, MA), and the membrane was exposed to x-ray film (Kodak).

To demonstrate the integrity and total amount of RNA electrophoresed, the membrane was stripped, hybridized with the biotin-labeled 28S probe, and used for detection as above.

Statistical Analysis

For each adult kidney studied, the degree of cortical interstitial macrophage infiltration and cortical tubular osteopontin expression was determined and plotted on a scattergram. The statistical significance of the data was analyzed using the Spearman rank correlation coefficient (Spearman's rho) of nonparametric data. Significance was defined as $P < 0.05$.

Results

Human Fetal Kidney

Immunohistochemistry. Osteopontin protein is uniformly expressed by a subset of tubular structures in the fetal kidney. The intensity of the immunohistochemical staining, a rough measure of the amount of protein present, appears to increase with increasing age of the fetus. In the kidneys from gestational age 54 d through approximately 80 d, tubules stain very weakly and essentially exclusively along the luminal surfaces of the tubules (Figure 1, A and B). A minority of ureteric bud structures demonstrate similar, weak expression of osteopontin at the luminal surface. Other structures, including blastema, developing glomeruli, interstitial cells, vascular structures, and urothelium demonstrate no detectable expression of osteopontin at this time point.

There is a striking and uniform change in osteopontin expression in fetal kidneys of greater than 80 d gestation. This change is not primarily an altered pattern of expression, but one whereby the intensity of staining in tubular structures is increased and frequently reveals the presence of osteopontin throughout the tubular cell cytoplasm rather than confined to

Table 1. Pattern of osteopontin immunostaining in human fetal kidney

Gestational Age (days)	Number Studied	Ureteric Bud Staining	Tubular Staining	Glomerular Staining
54 to 57	5	Negative	Faint, luminal positivity	Negative
59	1	Positive on luminal tip	Faint, luminal positivity	Negative
67	1	Negative	Faint, luminal positivity	Negative
72	2	Faint, luminal positivity	Faint, luminal positivity	Negative
73	2	Positive	One faint positive, one strong positive	Negative
75	1	Positive	Strong positive	Negative
76	1	Negative	Moderate positive	Negative
81	3	Positive	Strong positive	One with positive parietal epithelium, others negative
84	1	Negative	Strong positive	Negative
89	2	Faint, luminal positivity	Strong positive	One with positive parietal epithelium, others negative
96 to 127	6	Negative	Strong positive	Negative

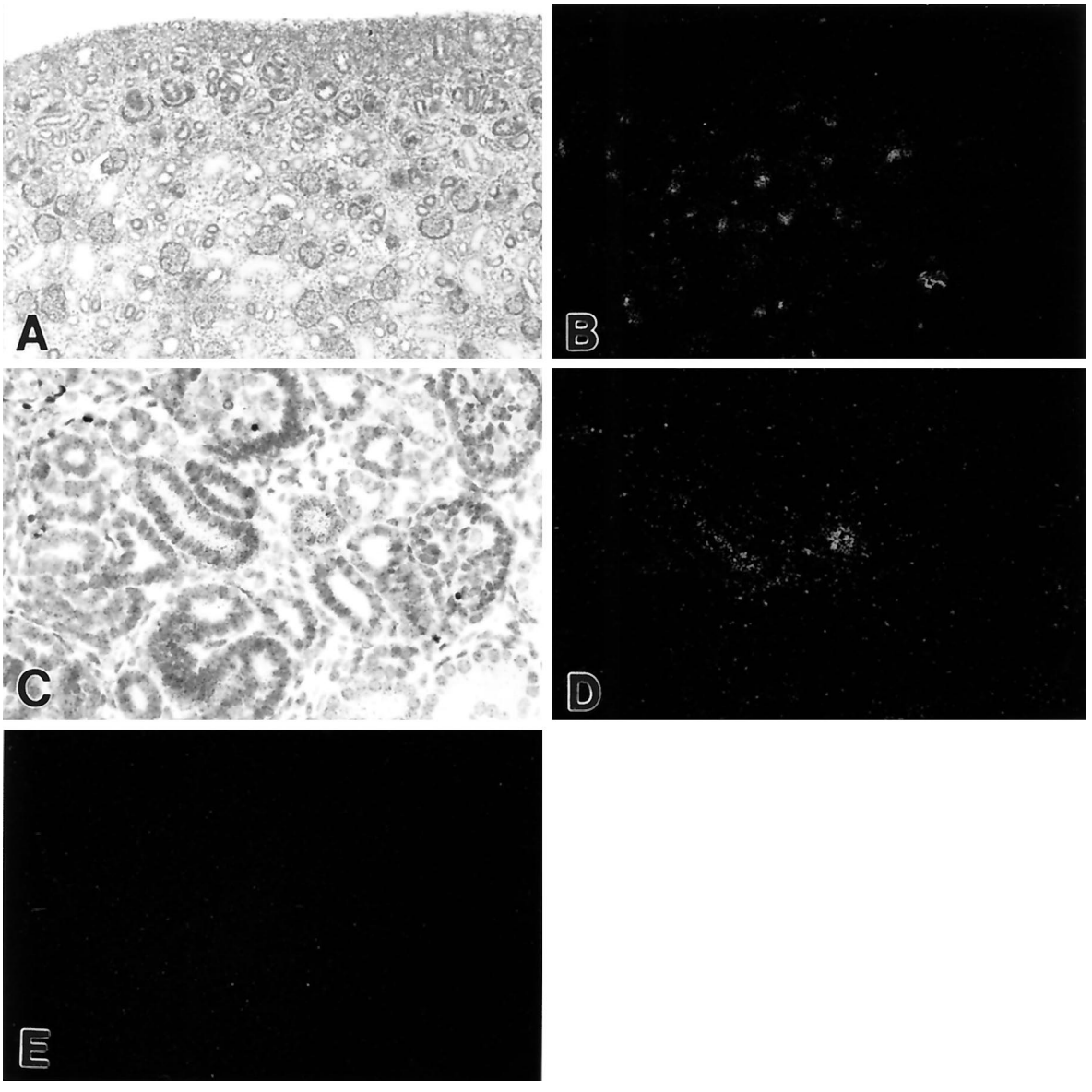

Figure 2. Demonstration of osteopontin mRNA in human fetal kidney by *in situ* hybridization. (A and B) Low-power view of 94-d fetal kidney hybridized with the 35S-labeled antisense osteopontin riboprobe, demonstrating strong mRNA expression in tubular segments. Light (A) and dark-field (B) photomicrographs of the same microscopic field. (C and D) Higher power view of the same kidney shown in A and B above. Osteopontin mRNA expression can be seen localized to two tubular segments, with no expression by glomeruli or interstitial cells. Light (C) and dark-field (D) photomicrographs of same microscopic field. (E) Negative control section was hybridized with 35S-labeled sense osteopontin riboprobe. Dark-field photograph of same low-power view shown in A and B above. Magnification: ×100 in A, B, and E; ×400 in C and D.

Table 2. Gestational ages of fetal kidneys studied[a]

Gestational Age (days)	ICC	ISH	Northern Blotting
50 to 59	6	3	0
60 to 69	1	2	0
70 to 79	6	5	1
80 to 89	6	2	1
90 to 99	1	1	0
Over 100	5	0	0

[a] ICC, immunocytochemistry; ISH, *in situ* hybridization.

the luminal surface (Figure 1C). The enhanced tubular expression, while frequently widespread among all tubular segments present in the histologic sections, in some cases is found only in a proportion of cortical tubules within the sample. The limited differentiation of tubular segments at this time period, and the lack of segment-specific cell markers, precludes unequivocal determination of whether the focal expression of osteopontin is restricted to specific tubular segments in these cases. However, in some cases, positively stained tubules can be seen emerging from the glomeruli, which identifies the tubules as proximal segments (Figure 1E). There are also occasional osteopontin-expressing parietal epithelial cells lin-

ing Bowman's capsule. Osteopontin expression could be identified in some, but not all, of the ureteric buds present in the blastema, often demonstrating the same luminal localization pattern observed in fetal kidneys of the younger gestational age group (Figure 1D). A single fetal kidney of 81 d gestation exhibited osteopontin expression in a minority of S-shaped glomerular structures available for examination, but in general these older fetal kidneys demonstrated no detectable osteopontin expression in blastema, immature or differentiated glomeruli, the majority of interstitial cells, collecting ducts, or urothelium lining the fetal bladder. There was very strong expression of osteopontin in a small subset of cells found within the medullary interstitium and just under the capsule of the kidney. Beginning at approximately day 72, there was expression of osteopontin in the mesenchymal cells comprising the adventitia of the arterial vessels (Figure 1F), but no expression was seen in the vascular smooth muscle cells or endothelial surface of these vessels. A summary of the observed immunostaining pattern is presented in Table 1.

In Situ Hybridization. *In situ* hybridization localization of osteopontin mRNA in tissue sections was performed using both the ^{35}S-labeled riboprobe (Figure 2) and the digoxigenin-labeled riboprobe (data not shown). The results were consistent with those obtained by immunocytochemistry and Northern blotting, showing the strongest mRNA signals in tubular segments of the kidneys greater than 80 d gestation (Figure 2, A through E), and little or no detectable signal in younger kidneys (data not shown). Strong hybridization signal of scattered subcapsular and interstitial cells could also be seen, although the identity of these cells remains unknown. We studied a total of 25 fetal kidneys by immunohistochemistry, 13 by *in situ* hybridization and two by Northern blotting. These represented a range of gestational ages as shown in Table 2.

Northern Blotting. The distinct patterns of osteopontin expression between kidneys of less than 80 d gestation and those that are older, indicative of increased amounts of osteopontin in the more developed kidneys observed by immunohistochemical and *in situ* hybridization studies, was supported by complementary studies of osteopontin mRNA within these tissues as assessed by Northern blotting. In these studies, hybridization to blots of whole kidney mRNA revealed very weakly detectable (by this technique) osteopontin mRNA in a kidney of 72 d gestation. More developed kidneys revealed increased production of osteopontin RNA, with a very strong band detected in the age 85 d kidney (Figure 3).

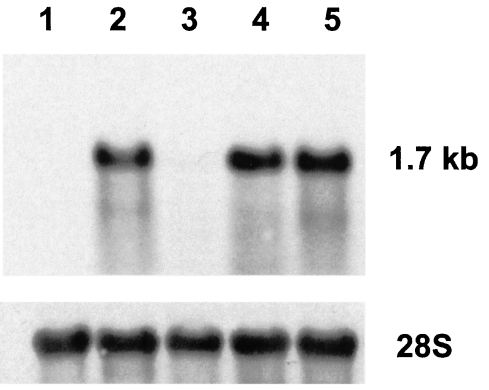

Figure 3. Northern blot of total human kidney RNA. Northern blot using biotin-labeled riboprobe to osteopontin. Lane 1, 72-d fetal kidney; lane 2, 85-d fetal kidney; lane 3, adult kidney 1; lane 4, adult kidney 2; lane 5, adult kidney 3. There are faint, barely detectable bands at 1.7 kb in lanes 1 and 3, which are not readily seen at the level of exposure that permits delineation of distinct bands seen in lanes 2, 4, and 5. Shown below the Northern blot is the same membrane hybridized with a biotin-labeled 28S riboprobe, demonstrating the approximate relative concentration of total RNA loaded and the integrity of the RNA used.

Human Adult Kidney

Immunohistochemistry. In the human adult kidney, osteopontin is uniformly expressed by a subset of distal tubules. All of the cases studied demonstrated osteopontin positivity in the distal nephron, although the total number of positive tubular cross sections varied widely. Immunostaining for osteopontin is especially strong in what appear to be the thick ascending limb of the loop of Henle (Figure 4A), based on the morphologic appearance of low columnar cells and a lack of brush border. The immunostaining in the distal tubular segments appears cytoplasmic at the light microscopic level. By immunoelectron microscopy, osteopontin immunoreactivity was localized primarily to the luminal surface of distal tubular segments, with focal immunostaining seen within the cytoplasm (Figure 5). The cytoplasmic staining appears to be associated with the Golgi apparatus and possibly the endoplasmic reticulum, as well as some possible lysosomal structures. Staining for osteopontin could also be seen occasionally in individual cells of the collecting duct (Figure 4B), although the vast majority of collecting ducts present in the tissues studied demonstrated no specific expression. Staining of the proximal tubular segments varied greatly among the tissue sections used in this study, from very little or no staining to widespread strong staining. When the proximal tubules demonstrated expression of osteopontin protein, the staining was very punctate and was seen in a distinct perinuclear pattern (Figure 4C). In those kidneys in which proximal tubular expression was identified, there was uniform staining of all cells comprising the tubular segments present in the histologic section.

Due to the heterogeneity and the limited availability of human tissue, it is difficult to definitively determine the degree and localization of osteopontin expression in "normal" adult kidney. In this study, we used portions of kidneys resected for localized tumors that were macroscopically and microscopically uninvolved by the neoplastic process. We cannot rule out the possibility that presence of the malignancy contributed to the observed osteopontin expression or macrophage infiltration.

In Situ Hybridization. Results of the *in situ* hybridization for osteopontin mRNA expression closely mirrored those seen by immunocytochemistry, with distal segments of the nephron showing positive signal in all tissue sections studied and a wide range of expression exhibited by the proximal tubules (Figure 6, A through D). The antibody LF7 is also reactive in formalin-

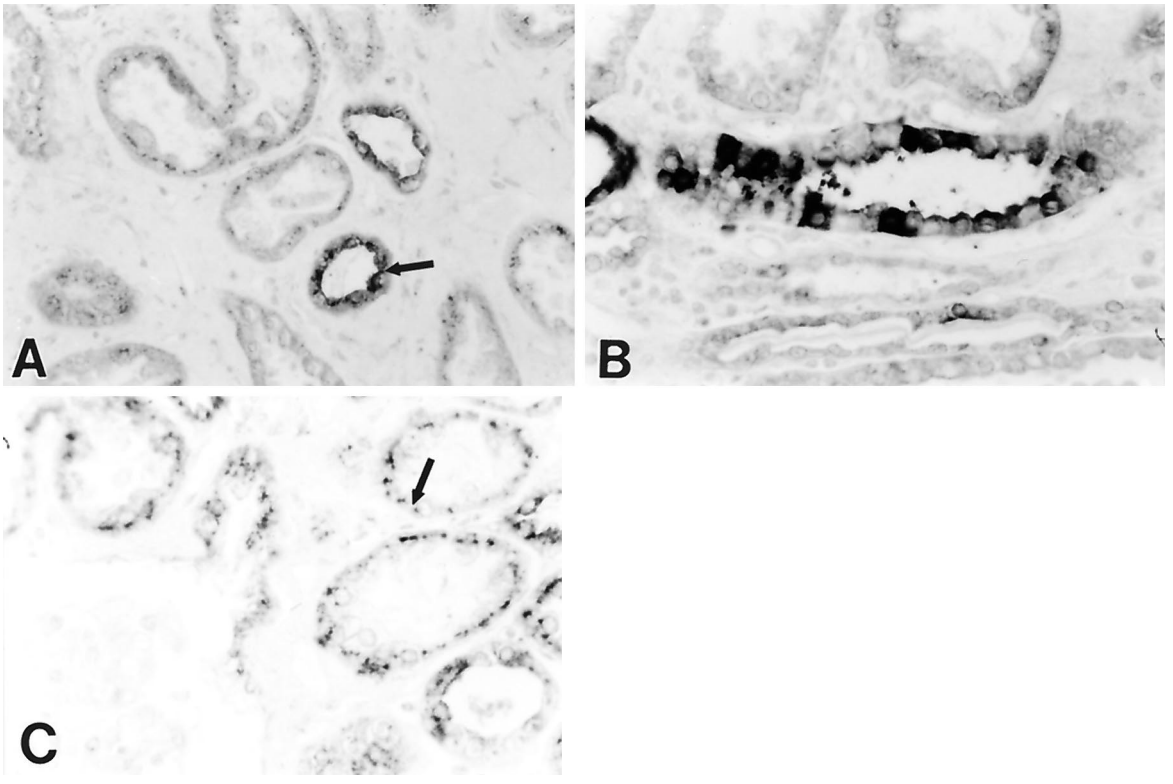

Figure 4. Immunocytochemical demonstration of osteopontin expression in adult human kidney. (A) Osteopontin is constitutively expressed in distal tubules of adult human kidney (arrow). (B) Osteopontin is expressed in individual cells of the collecting duct in some kidney sections. (C) Expression of osteopontin is seen in the proximal tubules of some adult kidneys. This expression is usually seen in a very distinct, perinuclear pattern (arrow). Magnification: ×600 in A through C.

Figure 5. Immunoelectron microscopy of a mature adult distal tubule. Osteopontin immunostaining is very strong at the luminal surface of the tubule, but there is also focal expression seen in lysosomal structures (arrow) and near the basal surface, possibly associated with the Golgi apparatus (arrowheads). Magnification: ×2100.

fixed tissue, and so replicate sections were used for immunocytochemistry and *in situ* hybridization with the digoxigenin-labeled probe. As can be seen in Figure 6, E and F, the patterns of localization of osteopontin protein and mRNA are very similar.

Northern Blotting. The heterogeneity of osteopontin expression in our nephrectomy tissues is also demonstrated by Northern blotting (Figure 3), which clearly shows that some kidneys, although classified as normal, contain a great deal of osteopontin mRNA, while other express very little. Quantitatively, adult kidney 1 (lane 3) had 13% of the total tubular population osteopontin positive, whereas adult kidney 2 (lane 4) had 86% positive and adult kidney 3 (lane 5) had 91% positive. Osteopontin immunostaining of adult kidney 2 can be seen in Figure 7, A and B, and osteopontin expression in adult kidney 3 is shown in Figure 4C.

Correlation of Osteopontin Expression and Macrophage Infiltrate. In the adult renal tissue sections used in this study, which are primarily obtained from older patients and generally come from kidneys resected for localized neoplasms, there is a wide range of "normal" phenotype of kidney uninvolved by tumor and located at a distance from the tumor margins. Many of these tissues have mild-to-moderate degrees of interstitial fibrosis, which has a well established association with aging. Most also have the mild focal interstitial inflammation that is almost invariably encountered in areas of interstitial fibrosis. To examine these factors, tissue sections were stained with anti-α-smooth muscle actin and with anti-CD68 antibodies to demonstrate interstitial myofibroblasts and macrophages, re-

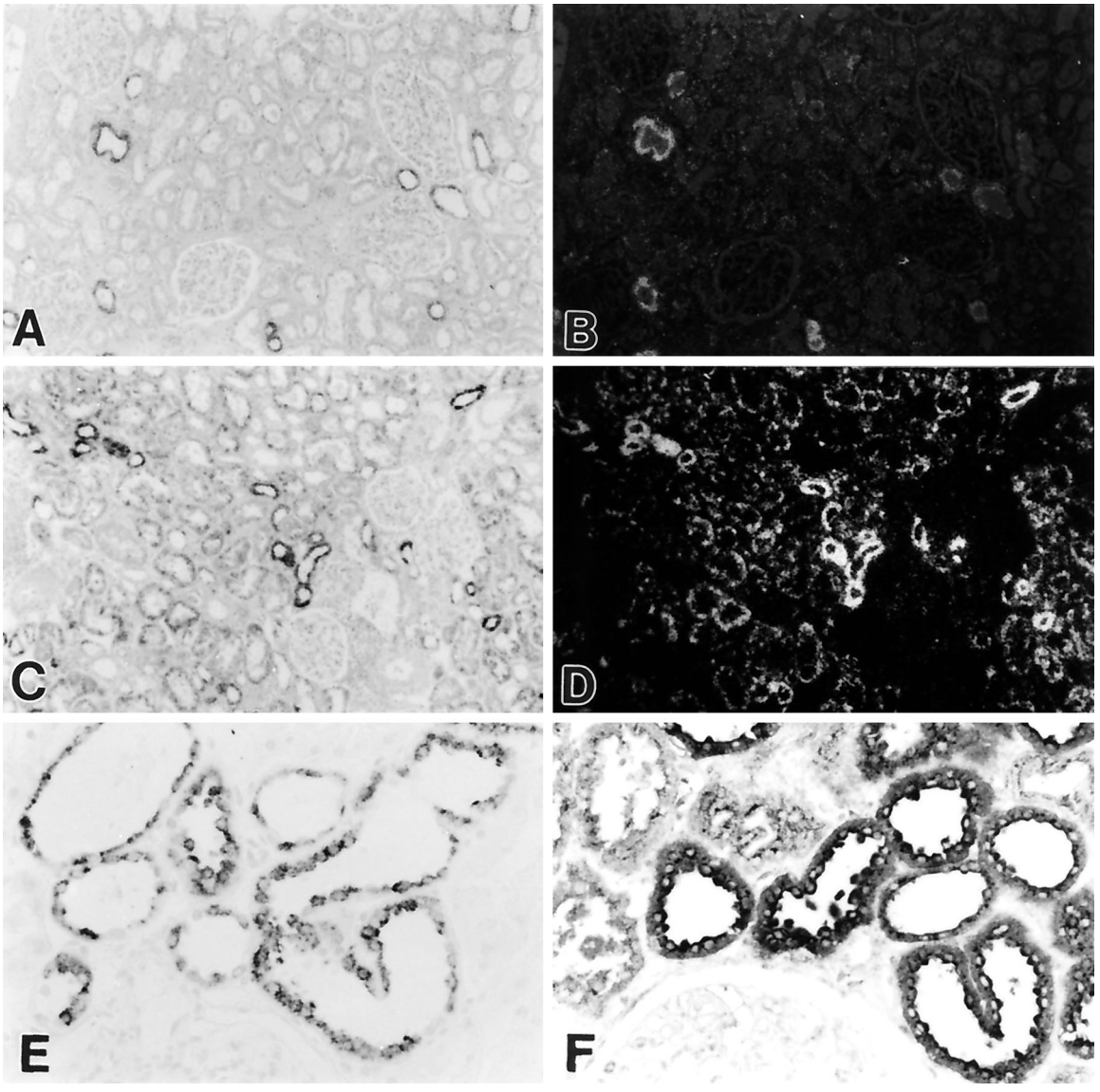

Figure 6. Protein and mRNA expression in adult human kidney demonstrated by *in situ* hybridization and immunohistochemistry. (A and B) *In situ* hybridization of a normal adult kidney using ^{35}S-UTP labeled riboprobe demonstrating localization of osteopontin mRNA to distal tubules. Light (A) and dark-field (B) photomicrographs of same field. (C and D) *In situ* hybridization (^{35}S-labeled riboprobe) of an adult kidney exhibiting foci of interstitial fibrosis. Osteopontin mRNA is widespread, showing strong localization in distal tubules and distinct but lesser signal in the proximal tubules. Light (C) and dark-field (D) photomicrographs of same field. (E) *In situ* hybridization of the same tissue section shown in A, using a digoxigenin-labeled riboprobe instead of a radiolabeled riboprobe. A similar pattern of mRNA localization in the distal tubules is demonstrated regardless of whether radioactive isotopes or digoxigenin labels are used as the test system for analysis. (F) Immunohistochemical staining of same adult kidney as shown in E with antibody LF7, showing osteopontin protein expression generally confined to the distal tubules, corresponding to patterns of osteopontin synthesis demonstrated by *in situ* hybridization. Magnification: ×100 in A through D; ×400 in E and F.

spectively. All of the tissue sections were examined in a blinded manner. Using a magnification of ×400, 10 random cortical fields were counted for positive expression of osteopontin in tubular cross sections and, on a separate serial section, 10 equivalent random fields were counted for CD68-positive cells. The quantitative data on the extent of interstitial macrophage infiltrate and osteopontin expression present in the adult kidneys used for this study are presented as a scattergram in Figure 8. In individual tissue sections, the number of osteopontin-positive tubular segments correlated strongly with the degree of interstitial macrophage accumulation (rho = 0.793; $P < 0.005$). Two representative cases are shown in Figure 7, demonstrating that increased tubular osteopontin expression correlates with the degree of macrophage infiltrate present in the tissue. The degree of smooth muscle actin-positive cells present in the interstitium was graded semiquantitatively, as outlined in Materials and Methods. There was no significant correlation between actin staining and osteopontin expression (data not shown). There was no correlation between the patient age and the degree of osteopontin expression.

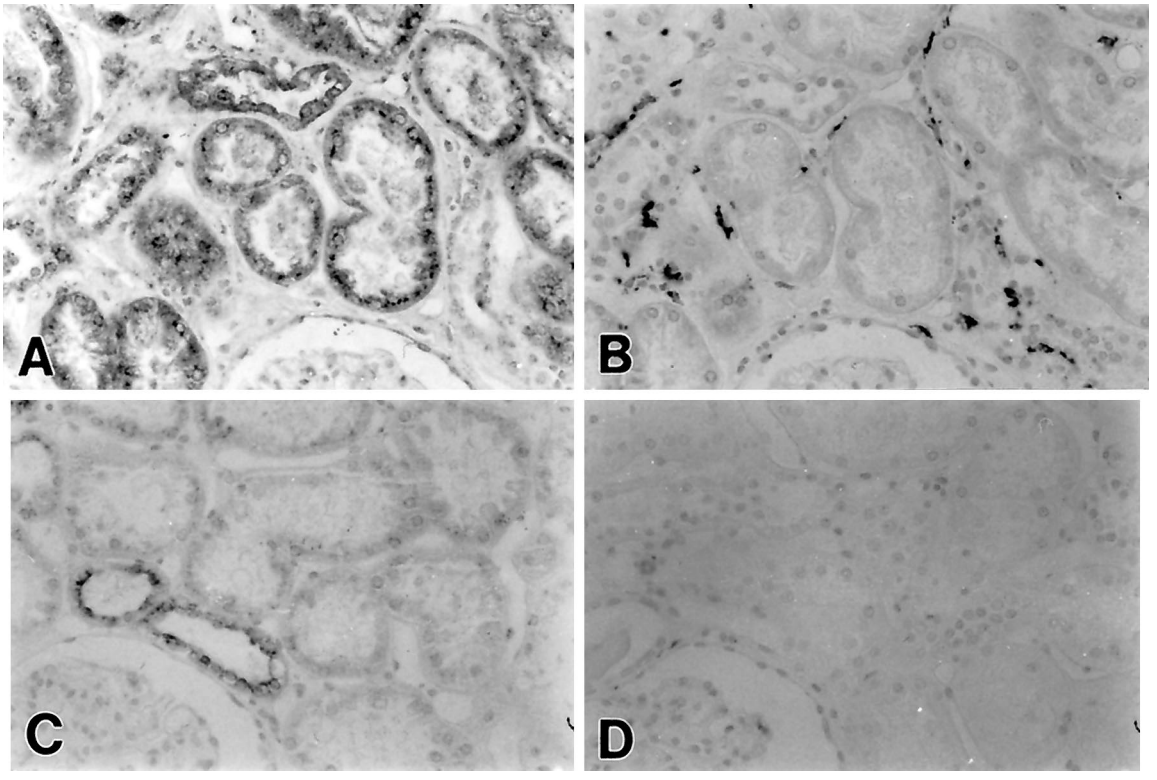

Figure 7. Comparison of osteopontin expression and the presence of CD68-positive macrophages. (A) Osteopontin expression in adult human kidney with tubulointerstitial fibrosis. Osteopontin is expressed by nearly all tubules present in the cortex. (B) Staining of serially sectioned tissue from the same specimen as A with anti-CD68 antibody, demonstrating widespread presence of interstitial macrophages. (C) Normal adult kidney with no expression of osteopontin in proximal tubular epithelium. Osteopontin immunoreactivity can be seen in two distal tubular segments directly adjacent to the glomerulus. (D) Serially sectioned tissue from the same specimen as C, stained with anti-CD68 antibody, showing essentially no macrophages present in the interstitium. Magnification: ×400 in A through D.

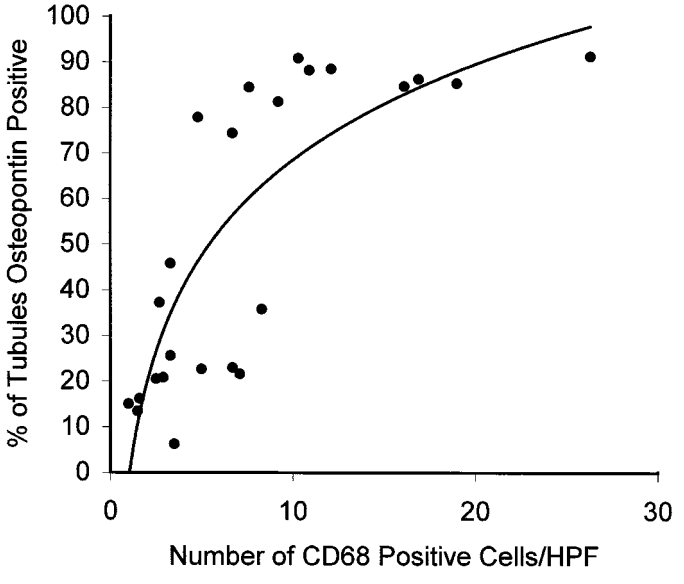

Figure 8. Comparison of tubular osteopontin expression with monocyte infiltration of adjacent interstitium (rho = 0.793; $P < 0.005$).

Identification of Osteopontin-Positive Tubules. Double immunohistochemistry demonstrated colocalization of osteopontin and EMA in distal tubular segments (Figure 9A). This pattern of expression was confirmed by double immunolabeling with the anti-Na,K-ATPase antibody (Figure 9B). Immunostaining of serial sections showed a similar colocalization of osteopontin, EMA, and Na,K-ATPase in the distal nephron (Figure 10, A through C) in a kidney that had less that 25% of the total tubular segments present positive for osteopontin. In a kidney that had greater than 90% of the total tubular segments osteopontin-positive, staining for osteopontin can be observed in all tubular segments (Figure 10D), including proximal tubular segments. Although not apparent in the photograph, due to the methyl green counterstain used, many of the osteopontin-positive tubules shown have a visible brush border. Serial sections were immunostained with EMA and Na,K-ATPase (Figure 10, E and F) to further localize portions of the distal nephron. Thus, osteopontin expression could be found in many, but not all, segments of the distal nephron in every tissue studied. In some cases, punctate perinuclear staining for osteopontin occurs in proximal tubular segments that were negative for both EMA and Na,K-ATPase.

Discussion

In this study, we describe the localization and expression of osteopontin in the normal developing and adult human kidney. Osteopontin expression in the human fetal kidney closely correlates with patterns of localization seen in the developing

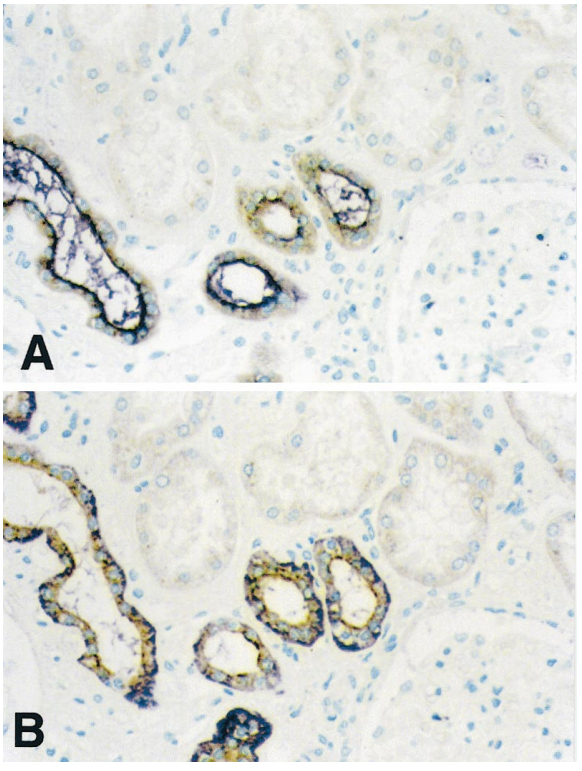

Figure 9. Double immunohistochemistry for osteopontin and markers of distal tubules. (A) Distal tubules produce osteopontin as shown by double labeling with antibodies to osteopontin (brown) and epithelial membrane antigen (EMA) (purple). (B) Replicate tissue section of that shown in A, demonstrating double labeling of the same distal tubules with osteopontin (brown) and Na,K-ATPase (purple) antibodies. Magnification: ×400 in A and B.

mouse and rat (10,24), although we did identify a differential expression of the molecule depending on the gestational age of the human fetal kidney. Osteopontin protein and mRNA expression are significantly upregulated at approximately day 75 to 80 of gestation. In the adult human kidney, expression of osteopontin protein and mRNA is very heterogeneous, ranging from expression only in a subset of the distal nephron to widespread expression in all tubular segments. Localized expression of osteopontin correlates well with the number of interstitial macrophages present in the same tissue locations.

Osteopontin was originally isolated from bone and was thought to be a bone-specific protein (6). More recently, osteopontin has been localized in a number of other tissues, including kidney (2,10,22,24,26), and appears to be widely associated with the luminal surfaces of epithelial cells in a number of organs (1). Osteopontin expression has been demonstrated in the developing mouse and rat kidney (10,16,24), as well as in normal and diseased adult rat kidneys (20–22,26–28,43). Reports of the precise cellular localization of osteopontin within the rodent kidney have been somewhat conflicting. Studies in normal mouse kidney localized osteopontin protein to the thick ascending limb of the loop of Henle and the distal tubules (44), while another group reported localization of osteopontin mRNA in both proximal and distal tubules and loops of Henle in developing mouse kidney (10). Studies in normal rat demonstrate osteopontin protein and mRNA localized to the thin limb of Henle and papillary surface epithelium (26,45), distal tubules (8,22), parietal epithelial cells (22), and collecting duct (22). In these studies, there was no report of osteopontin in proximal tubules of a normal kidney. There are a number of reports of upregulation of osteopontin expression in cortical tubules in renal disease models (15,19–22,27,28,43). Immunoelectron microscopic studies have also been somewhat conflicting. Osteopontin protein has been localized to the Golgi apparatus and cytoplasmic vesicles in the thin limb and distal tubular epithelium and to the vacuolar-lysosomal system in proximal tubules of rat kidney (26), to secretory vesicles that were distinct from lysosomes and endosomes in rat papillary surface epithelium (45), and to the phagolysosomes in the absorptive epithelial cells of rat small intestine (46).

In contrast to these studies, very little is known about the localization of osteopontin in human kidney, with the exception of one report that surveyed a wide range of tissues and demonstrated the localization of osteopontin protein and mRNA in distal tubules, collecting duct, and transitional epithelium of the renal pelvis (1). To extend the observations of osteopontin expression seen in rodent models of renal disease and development to the human state, it is imperative to precisely localize osteopontin in human kidney.

Expression of osteopontin in the human fetal kidney appears to be developmentally regulated. There is very low expression of both mRNA (by Northern blotting and *in situ* hybridization) and peptide product (by immunohistochemistry) in kidneys of less than 75 d gestation, compared with upregulated expression detected in kidneys of approximately 80 d gestation and older. The increased immunostaining seen in the kidneys older than 80 d does not represent simply an increase in absorption of osteopontin protein from the developing fetus' urine, since a corresponding increase was shown to occur in mRNA expression, indicative of active synthesis, by *in situ* hybridization and Northern blotting. This agrees with data in developing rat kidney, in which a marked increase in osteopontin RNA was seen in day 21 *versus* day 14 embryonic rat kidney (10,24). The questions of how osteopontin functions in human nephrogenesis and why its expression appears to be turned on or significantly upregulated at approximately 80 d gestation remains an enigma.

The most striking demonstration of the potential importance of osteopontin in orderly tubular development comes from studies of a rat metanephric organ culture system, where it has been demonstrated that osteopontin expression is essential for normal tubulogenesis to occur (16). In this system, when osteopontin activity was blocked with neutralizing antibody or when the $\alpha v\beta 3$ receptor for osteopontin was inhibited by binding with specific antibody or with a competing RGD peptide, the tubules failed to develop normally and showed increased apoptosis. This finding suggests that osteopontin functions, at least in part, as a survival factor for renal tubular epithelium during development. In another study, αv integrin peptide-antisense oligodeoxynucleotide or antibody specific for αv was introduced to a metanephric culture, resulting

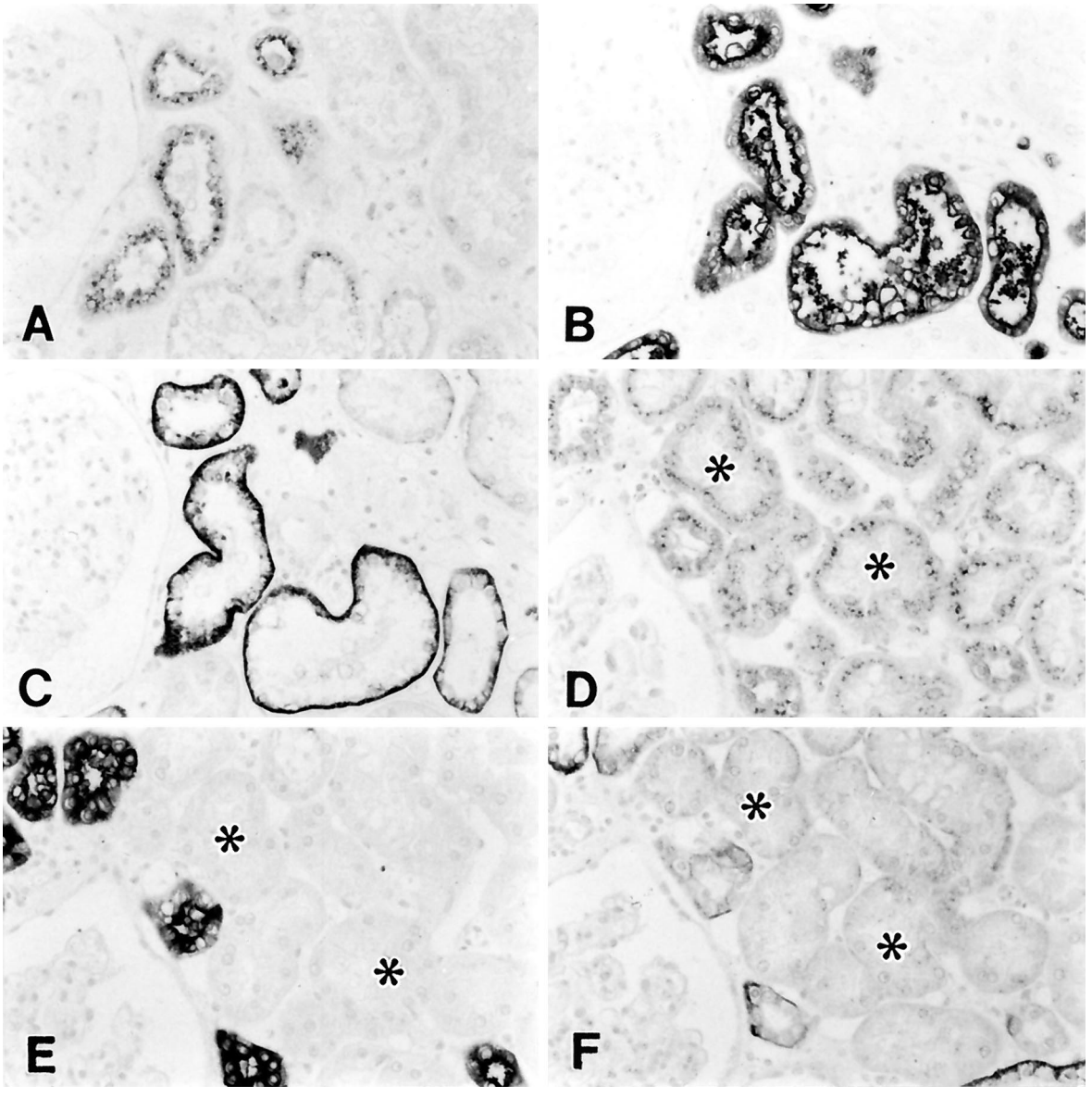

Figure 10. Immunolocalization of osteopontin, EMA, and Na,K-ATPase. (A through C) Osteopontin (A), EMA (B), and Na,K-ATPase (C) expression in serial sections of a kidney demonstrating low expression of osteopontin (21% of tubular segments are osteopontin-positive). Osteopontin immunoreactivity is confined to distal tubular segments that are also positive for both EMA and Na,K-ATPase. (D through F) Osteopontin (D), EMA (E), and Na,K-ATPase (F) expression in serial sections from a kidney demonstrating high expression of osteopontin (91% of tubular segments are osteopontin-positive). Osteopontin expression is seen in virtually all tubular segments shown, including proximal tubules, which are negative for both EMA and Na,K-ATPase (asterisks). Although not apparent in the photograph due to the counterstain used, the tubular segments marked with asterisks had a brush border that could be identified under the microscope. Magnification: ×400 in A through F.

significant disruption of kidney development (47). αv integrin is expressed in the mouse beginning at day 13 of gestation, and its expression increases progressively in the fetal and neonatal kidney (47). From these studies, it would appear that osteopontin and its interaction with the $\alpha v\beta 3$ integrin is an important mediator of normal tubulogenesis, and that both are spatiotemporally expressed during nephrogenesis. However, osteopontin is not absolutely required for normal tubulogenesis, as it has been observed that kidneys in osteopontin knockout mice develop normally, without apparent defects (48). This indicates that there are alternate mechanisms that allow the kidney to develop in the absence of osteopontin.

There are several postulated *in vivo* functions for osteopontin in the adult kidney. Osteopontin has been shown to block calcium oxalate crystal formation (49) and block adhesion of calcium oxalate crystals to cultured renal epithelial cells (50). In urine obtained from patients with kidney stones, however, no significant difference in the levels of urinary osteopontin could be found when compared with control subjects, although the patients did have an increase in the level of low molecular

weight variants of osteopontin compared with the healthy subjects (51). Thus, in functionally normal kidneys, intact osteopontin may act to inhibit the formation and binding of calcium oxalate crystals found in the urine and thereby inhibit stone formation.

Our group and others have shown that tubular osteopontin expression is significantly increased in several rat models of renal disease, which mirror human disease, including the Thy-1 model of mesangial proliferative nephropathy (22), the aminonucleoside nephrosis model of minimal change disease (22,27), the passive Heymann nephritis model of membranous nephropathy (22), cyclosporine nephropathy (21,23), and angiotensin II-induced tubulointerstitial nephritis (20). These studies all show an influx of macrophages following the early increased expression of osteopontin and the tendency of macrophages to localize near tubules expressing osteopontin. Osteopontin expression by renal tubules is also increased by conditions that induce proteinuria and lead to interstitial inflammation and fibrosis (43), and in kd/kd mice that spontaneously develop tubulointerstitial nephritis (15). These studies, coupled with others showing that a subcutaneous injection of osteopontin leads to a cellular infiltrate that is primarily composed of macrophages (52), strongly suggest that osteopontin plays a proinflammatory role by promoting the recruitment of macrophages to sites of tubulointerstitial injury in the kidney. Consistent with this hypothesis, neutralizing antibodies directed against osteopontin blocked macrophage infiltration in a rat dermal inflammation model (40). Additionally, in a model of ureteral obstruction, osteopontin knockout mice demonstrate a decrease in renal macrophage infiltrate and an increase in tubular epithelial cell apoptosis when compared with wild-type mice (48).

In the present study, we demonstrate that osteopontin is constitutively expressed in a subset of the human distal nephron. In addition, we show that osteopontin expression can be seen to be locally upregulated in human kidneys at sites that exhibit interstitial inflammation and fibrosis. The extent of expression of osteopontin in individual samples of renal cortex correlates to the degree of interstitial macrophage infiltrate, further strengthening the proposed role of osteopontin as a proinflammatory molecule in the kidney. In addition to this role as a chemoattractant for monocytes and macrophages, the expression of osteopontin in the adult human kidney may also serve as a proinflammatory stimulus by mediating nitric oxide signaling (53,54) and may serve a protective role for epithelial cells against stimuli promoting apoptosis.

Acknowledgments

This work was supported by an O'Brien Kidney Center grant (National Institutes of Health [NIH] Grant DK47659) and National Science Foundation Grant EEC9529161. We thank the Central Laboratory for Human Embryology at the University of Washington (supported by Grant HD 00836 from NIH) for assistance in providing fetal tissue.

References

1. Brown LF, Berse B, Van de Water L, Papadopoulos-Sergiou A, Perruzzi CA, Manseau EJ, Dvorak HF, Senger DR: Expression and distribution of osteopontin in human tissues: Widespread association with luminal epithelial surfaces. *Mol Biol Cell* 3: 1169–1180, 1992
2. Butler WT: The nature and significance of osteopontin. *Connect Tissue Res* 23: 123–136, 1989
3. Murry CE, Giachelli CM, Schwartz SM, Vracko R: Macrophages express osteopontin during repair of myocardial necrosis. *Am J Pathol* 145: 1450–1462, 1994
4. Giachelli C, Bae N, Lombardi D, Majesky M, Schwartz S: Molecular cloning and characterization of 2B7, a rat mRNA which distinguishes smooth muscle cell phenotypes in vitro and is identical to osteopontin (secreted phosphoprotein I, 2aR). *Biochem Biophys Res Commun* 177: 867–873, 1991
5. Giachelli CM, Liaw L, Murry CE, Schwartz SM, Almeida M: Osteopontin expression in cardiovascular diseases. *Ann NY Acad Sci* 760: 109–126, 1995
6. Oldberg A, Franzen A, Heinegard D: Cloning and sequence analysis of rat bone sialoprotein (osteopontin) cDNA reveals an Arg-Gly-Asp cell-binding sequence. *Proc Natl Acad Sci USA* 83: 8819–8823, 1986
7. Patarca R, Freeman GJ, Singh RP, Wei FY, Durfee T, Blattner F, Regnier DC, Kozak CA, Mock BA, Morse HC, Jerrells TR, Cantor H: Structural and functional studies of the early T lymphocyte activation 1 (Eta-1) gene: Definition of a novel T cell-dependent response associated with genetic resistance to bacterial infection. *J Exp Med* 170: 145–161, 1989
8. Kohri K, Nomura S, Kitamura Y, Nagata T, Yoshioka K, Iguchi M, Yamate T, Umekawa T, Suzuki Y, Sinohara H, Kurita T: Structure and expression of the mRNA encoding urinary stone protein (osteopontin). *J Biol Chem* 268: 15180–15184, 1993
9. Shiraga H, Min W, VanDusen WJ, Clayman MD, Miner D, Terrell CH, Sherbotie JR, Foreman JW, Przysiecki C, Neilson EG, Hoyer JR: Inhibition of calcium oxalate crystal growth in vitro by uropontin: Another member of the aspartic acid-rich protein superfamily. *Proc Natl Acad Sci USA* 89: 426–430, 1992
10. Nomura S, Wills AJ, Edwards DR, Heath JK, Hogan BL: Developmental expression of 2ar (osteopontin) and SPARC (osteonectin) RNA as revealed by in situ hybridization. *J Cell Biol* 106: 441–450, 1988
11. Uede T, Katagiri Y, Iizuka J, Murakami M: Osteopontin, a coordinator of host defense system: A cytokine or an extracellular adhesive protein? *Microbiol Immunol* 41: 641–648, 1997
12. Denhardt DT, Guo X: Osteopontin: A protein with diverse functions. *FASEB J* 7: 1475–1482, 1993
13. Hu DD, Lin EC, Kovach NL, Hoyer JR, Smith JW: A biochemical characterization of the binding of osteopontin to integrins alpha v beta 1 and alpha v beta 5. *J Biol Chem* 270: 26232–26238, 1995
14. Liaw L, Skinner MP, Raines EW, Ross R, Cheresh DA, Schwartz SM, Giachelli CM: The adhesive and migratory effects of osteopontin are mediated via distinct cell surface integrins: Role of alpha v beta 3 in smooth muscle cell migration to osteopontin in vitro. *J Clin Invest* 95: 713–724, 1995
15. Sibalic V, Fan X, Loffing J, Wuthrich RP: Upregulated renal tubular CD44, hyaluronan, and osteopontin in kdkd mice with interstitial nephritis. *Nephrol Dial Transplant* 12: 1344–1353, 1997
16. Rogers SA, Padanilam BJ, Hruska KA, Giachelli CM, Hammerman MR: Metanephric osteopontin regulates nephrogenesis in vitro. *Am J Physiol* 272: F469–F476, 1997
17. Liaw L, Almeida M, Hart CE, Schwartz SM, Giachelli CM: Osteopontin promotes vascular cell adhesion and spreading and

is chemotactic for smooth muscle cells in vitro. *Circ Res* 74: 214–224, 1994
18. Liaw L, Lindner V, Schwartz SM, Chambers AF, Giachelli CM: Osteopontin and beta 3 integrin are coordinately expressed in regenerating endothelium in vivo and stimulate Arg-Gly-Asp-dependent endothelial migration in vitro. *Circ Res* 77: 665–672, 1995
19. Diamond JR, Kees-Folts D, Ricardo SD, Pruznak A, Eufemio M: Early and persistent up-regulated expression of renal cortical osteopontin in experimental hydronephrosis. *Am J Pathol* 146: 1455–1466, 1995
20. Giachelli CM, Pichler R, Lombardi D, Denhardt DT, Alpers CE, Schwartz SM, Johnson RJ: Osteopontin expression in angiotensin II-induced tubulointerstitial nephritis. *Kidney Int* 45: 515–524, 1994
21. Pichler RH, Franceschini N, Young BA, Hugo C, Andoh TF, Burdmann EA, Shankland SJ, Alpers CE, Bennett WM, Couser WG, Johnson RJ: Pathogenesis of cyclosporine nephropathy: Roles of angiotensin II and osteopontin. *J Am Soc Nephrol* 6: 1186–1196, 1995
22. Pichler R, Giachelli CM, Lombardi D, Pippin J, Gordon K, Alpers CE, Schwartz SM, Johnson RJ: Tubulointerstitial disease in glomerulonephritis: Potential role of osteopontin (uropontin). *Am J Pathol* 144: 915–926, 1994
23. Young BA, Burdmann EA, Johnson RJ, Alpers CE, Giachelli CM, Eng E, Andoh T, Bennett WM, Couser WG: Cellular proliferation and macrophage influx precede interstitial fibrosis in cyclosporine nephrotoxicity. *Kidney Int* 48: 439–448, 1995
24. Chen J, Singh K, Mukherjee BB, Sodek J: Developmental expression of osteopontin (OPN) mRNA in rat tissues: Evidence for a role for OPN in bone formation and resorption. *Matrix* 13: 113–123, 1993
25. Liang CT, Barnes J: Renal expression of osteopontin and alkaline phosphatase correlates with BUN levels in aged rats. *Am J Physiol* 269: F398–F404, 1995
26. Madsen KM, Zhang L, Abu Shamat AR, Siegfried S, Cha JH: Ultrastructural localization of osteopontin in the kidney: Induction by lipopolysaccharide. *J Am Soc Nephrol* 8: 1043–1053, 1997
27. Magil AB, Pichler RH, Johnson RJ: Osteopontin in chronic puromycin aminonucleoside nephrosis. *J Am Soc Nephrol* 8: 1383–1390, 1997
28. Pichler R, Giachelli C, Young B, Alpers CE, Couser WG, Johnson RJ: The pathogenesis of tubulointerstitial disease associated with glomerulonephritis: The glomerular cytokine theory. *Miner Electrolyte Metab* 21: 317–327, 1995
29. Fleming S, Lindop GB, Gibson AA: The distribution of epithelial membrane antigen in the kidney and its tumours. *Histopathology* 9: 729–739, 1985
30. Holm-Nielsen P, Pallesen G: Expression of segment-specific antigens in the human nephron and in renal epithelial tumors. *Acta Pathol Microbiol Immunol Scand Suppl* 4: 48–55, 1988
31. Baskin DG, Stahl WL: Immunocytochemical localization of Na^+, K^+-ATPase in the rat kidney. *Histochemistry* 73: 535–548, 1982
32. Kashgarian M, Biemesderfer D, Caplan M, Forbush BD: Monoclonal antibody to Na,K-ATPase: Immunocytochemical localization along nephron segments. *Kidney Int* 28: 899–913, 1985
33. Alpers CE, Hudkins KL, Gown AM, Johnson RJ: Enhanced expression of "muscle-specific" actin in glomerulonephritis. *Kidney Int* 41: 1134–1142, 1992
34. Fisher LW, Hawkins GR, Tuross N, Termine JD: Purification and partial characterization of small proteoglycans I and II, bone sialoproteins I and II, and osteonectin from the mineral compartment of developing human bone. *J Biol Chem* 262: 9702–9708, 1987
35. Falini B, Flenghi L, Pileri S, Gambacorta M, Bigerna B, Durkop H, Eitelbach F, Thiele J, Pacini R, Cavaliere A, Martelli M, Cardarelli N, Sabattini E, Poggi S, Stein H: PG-M1: A new monoclonal antibody directed against a fixative-resistant epitope on the macrophage-restricted form of the CD68 molecule. *Am J Pathol* 142: 1359–1372, 1993
36. Skalli O, Ropraz P, Trzeciak A, Benzonana G, Gillessen D, Gabbiani G: A monoclonal antibody against alpha-smooth muscle actin: A new probe for smooth muscle differentiation. *J Cell Biol* 103: 2787–2796, 1986
37. Johnson RJ, Iida H, Alpers CE, Majesky MW, Schwartz SM, Pritzi P, Gordon K, Gown AM: Expression of smooth muscle cell phenotype by rat mesangial cells in immune complex nephritis: Alpha-smooth muscle actin is a marker of mesangial cell proliferation. *J Clin Invest* 87: 847–858, 1991
38. Heyderman E, Strudley I, Powell G, Richardson TC, Cordell JL, Mason DY: A new monoclonal antibody to epithelial membrane antigen (EMA)-E29. A comparison of its immunocytochemical reactivity with polyclonal anti- EMA antibodies and with another monoclonal antibody, HMFG-2. *Br J Cancer* 52: 355–361, 1985
39. Shyjan AW, Levenson R: Antisera specific for the alpha 1, alpha 2, alpha 3, and beta subunits of the Na,K-ATPase: Differential expression of alpha and beta subunits in rat tissue membranes. *Biochemistry* 28: 4531–4535, 1989
40. Giachelli CM, Lombardi D, Johnson RJ, Murry CE, Almeida M: Evidence for a role of osteopontin in macrophage infiltration in response to pathological stimuli in vivo. *Am J Pathol* 152: 353–358, 1998
41. Young MF, Kerr JM, Termine JD, Wewer UM, Wang MG, McBride OW, Fisher LW: cDNA cloning, mRNA distribution and heterogeneity, chromosomal location, and Rflp analysis of human osteopontin (Opn). *Genomics* 7: 491–502, 1990
42. Alpers CE, Hudkins KL, Ferguson M, Johnson RJ, Rutledge JC: Platelet-derived growth factor A-chain expression in developing and mature human kidneys and in Wilms' tumor. *Kidney Int* 48: 146–154, 1995
43. Eddy AA, Giachelli CM: Renal expression of genes that promote interstitial inflammation and fibrosis in rats with protein-overload proteinuria. *Kidney Int* 47: 1546–1557, 1995
44. Lopez CA, Hoyer JR, Wilson PD, Waterhouse P, Denhardt DT: Heterogeneity of osteopontin expression among nephrons in mouse kidneys and enhanced expression in sclerotic glomeruli. *Lab Invest* 69: 355–363, 1993
45. Kleinman JG, Beshensky A, Worcester EM, Brown D: Expression of osteopontin, a urinary inhibitor of stone mineral crystal growth, in rat kidney. *Kidney Int* 47: 1585–1596, 1995
46. Qu-Hong, Dvorak A: Ultrastructural localization of osteopontin immunoreactivity in phagolysosomes and secretory granules of cells in human intestine. *Histochem J* 29: 801–812, 1997
47. Wada J, Kumar A, Liu Z, Ruoslahti E, Reichardt L, Marvaldi J, Kanwar YS: Cloning of mouse integrin alphaV cDNA and role of the alphaV-related matrix receptors in metanephric development. *J Cell Biol* 132: 1161–1176, 1996
48. Ophascharoensuk V, Giachelli CM, Liaw L, Shankland SJ, Couser WG, Johnson RJ: Osteopontin (OPN) mediates early macrophage influx in renal interstitial inflammation: A study in OPN knockout (KO) mice [Abstract]. *J Am Soc Nephrol* 8: 481A, 1997

49. Hoyer JR, Otvos L Jr, Urge L: Osteopontin in urinary stone formation. *Ann NY Acad Sci* 760: 257–265, 1995
50. Lieske JC, Norris R, Toback FG: Adhesion of hydroxyapatite crystals to anionic sites on the surface of renal epithelial cells. *Am J Physiol* 273: F224–F233, 1997
51. Bautista DS, Denstedt J, Chambers AF, Harris JF: Low-molecular-weight variants of osteopontin generated by serine proteinases in urine of patients with kidney stones. *J Cell Biochem* 61: 402–409, 1996
52. Singh K, DeVouge MW, Mukherjee BB: Physiological properties and differential glycosylation of phosphorylated and non-phosphorylated forms of osteopontin secreted by normal rat kidney cells. *J Biol Chem* 265: 18696–18701, 1990
53. Hwang SM, Lopez CA, Heck DE, Gardner CR, Laskin DL, Laskin JD, Denhardt DT: Osteopontin inhibits induction of nitric oxide synthase gene expression by inflammatory mediators in mouse kidney epithelial cells. *J Biol Chem* 269: 711–715, 1994
54. Hwang SM, Wilson PD, Laskin JD, Denhardt DT: Age and development-related changes in osteopontin and nitric oxide synthase mRNA levels in human kidney proximal tubule epithelial cells: Contrasting responses to hypoxia and reoxygenation. *J Cell Physiol* 160: 61–68, 1994